A fast single image dehazing method based on statistical analysis

*Bui, Minh Trung, *방성배 **김원하
경희대학교
*minhtrung@khu.ac.kr, *sungbae9023@hanmail.net **wonha@khu.ac.kr

A fast single image dehazing method based on statistical analysis

*Bui, Minh Trung, *Seongbae Bang **Kim, Wonha
Kyung Hee University

*minhtrung@khu.ac.kr, *sungbae9023@hanmail.net, **wonha@khu.ac.kr

요약

In this paper, we propose a new single-image dehazing method. The proposed method constructs color ellipsoids that are statistically fitted to haze pixel clusters in RGB space and then calculates the transmission values through color ellipsoid geometry. The transmission values generated by the proposed method maximize the contrast of dehazed pixels, while preventing over-saturated pixels. The values are also statistically robust because they are calculated from the averages of the haze pixel values. Furthermore, rather than apply a highly complex refinement process to reduce halo or unnatural artifacts, we embed a fuzzy segmentation process into the construction of the color ellipsoid so that the proposed method simultaneously executes the transmission calculation and the refinement process. The results of an experimental performance evaluation verify that compared to prevailing dehazing methods the proposed method performs effectively across a wide range of haze and noise levels without causing any visible artifacts. Moreover, the relatively low complexity of the proposed method will facilitate its real-time applications.

1. Introduction

Many competitive single-image dehazing methods are based on the dichromatic model [1]-[9], which describes a hazy image as a mixture of the transmitted portion of the haze-free image and the portion of the light source that reaches the camera. Describing the dichromatic model in the RGB color space, the vectors of the hazier pixels are the more densely clustered. The dehazing methods based on the dichromatic model select a vector to indicate the extent to which pixel colors are diluted or hazed by the atmospheric light: that vector is named the prior vector. The prior vector could be selected from pixels [2], [3], [5], [9] or it could be calculated from the geometry of cluster distributions [1], [4], [6]. Those methods then linearly stretch the hazy vector cluster from the atmospheric light to each hazy vector until any become zeros [2]-[4] or the stretched prior color components of the stretched prior vector vector reaches to the origin [1], [6]. Thus, the selection of the prior vector determines the accuracy of transmission estimation and thereby the dehazing performance. When selecting the prior vector, its location, the randomness of the image signal, and the homogeneity of the image signal are all important factors.

Fig. 1 illustrates different dehazings with different prior vectors and shows the dehazing results. The prior vector P expands the hazy vector distribution less than the prior vector Q, which means that the

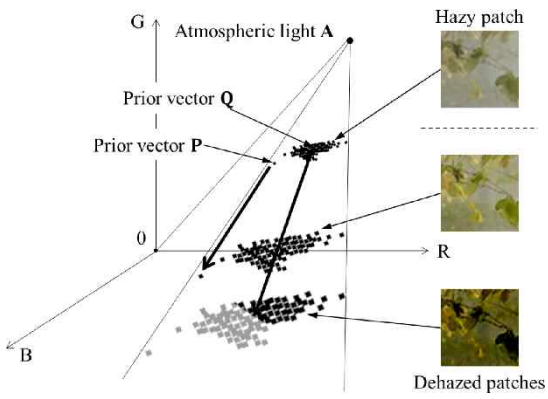

Fig. 1. Dehazing results by different prior vectors. The gray dots illustrate the over-saturated pixel vectors.

image dehazed by the prior vector P retains natural saturation but has lower contrast, while the one dehazed by the prior vector Q has higher contrast but also has the possibility of producing over-saturation, which usually appears as dark spots. To strike a balance between these results, each method for estimating transmission tries to set its prior vector

location to maximize the contrast of dehazed images while suppressing the over-saturation.

Because image signals are random, the signals from a local region may include irregular pixels that

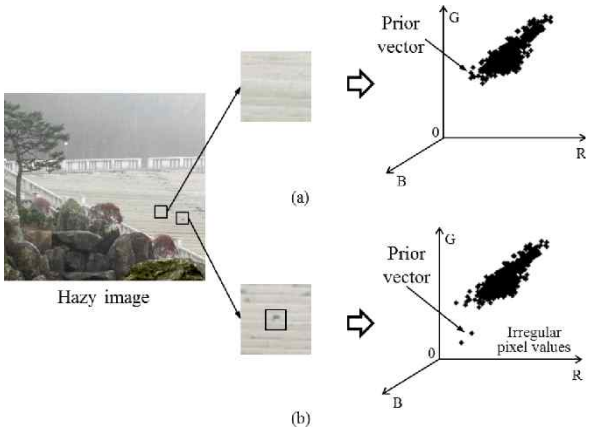

Fig. 2. Pixel value distributions of two nearby regions and their expected prior vectors. (a) Region without irregularly dark pixels, (b) region with irregular pixels.

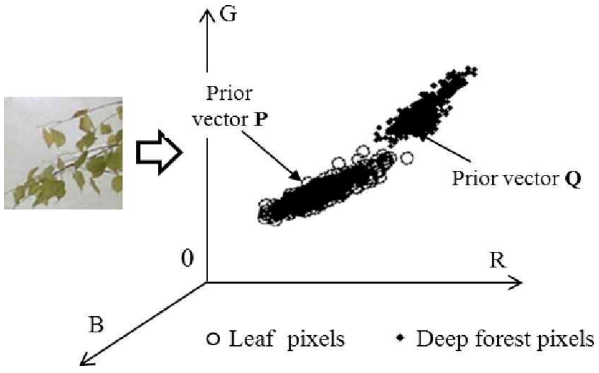

Fig. 3. Vector distribution of image patch including different regions, and the prior vector candidates.

are rarely correlated with the majority of pixels of the underlying local image. Fig. 2 shows

the distribution of pixel values for two nearby regions in a hazy image. Even if one region includes the irregular pixels that appear as small dark spots, these two proximate regions exhibit similar overall characteristics and equivalent degrees of haziness. However, when the prior vector is selected from among the irregular pixels, the dehazing result is insufficient because the prior vector is irrelevant to the majority of pixels and is closer to the origin. Therefore, the selection of the prior vector must also be statistically robust against signal randomness.

In a region across different objects, the vector cluster is combined from those objects, and so there exist multiple prior vectors that are appropriate for each object region. Fig. 3 illustrates the color vector distribution of a region that spans two different objects. There are two prior vector candidates: vectors P matching the leaves, and Q matching the deep forest. A prior vector selected from the mixed pixel vector distribution of the two object regions often produces a mismatch with one of the object regions, resulting in a halo artifact apparent along the strong edges [2], [4]. Alternatively, instead of selecting a prior vector from the mixed distribution of the heterogeneous region, the prior vector could be interpolated from prior vectors of neighboring homogeneous regions. However, the interpolated vector may not be relevant enough to the pixel vector distribution and may cause insufficient or excessive dehazing results [6].

2. Proposed color ellipsoid prior

The dichromatic model recovers the haze-free image from the hazy image at the location of such that [2], [6], [9],

$$\mathbf{x}_i = t_i \cdot \tilde{\mathbf{x}}_i + (1 - t_i) \cdot \mathbf{A} \qquad (1)$$

2.1 Color Ellipsoid Prior (CEP)

In the RGB color space, the vectors from hazier image signals are more densely clustered and normally distributed [4], [16]. The vector cluster region can be statistically approximated by an ellipsoid, where the shape of the ellipsoid is determined by the statistical moments of the vector distribution. An advantage of analyzing the ellipsoid is that it provides statistical robustness against random signals.

We denote as a vector variable in the RGB space. Let Ωi be the ellipsoid that fits the vector cluster region of the color pixels in . Then, can be constructed in the following manner [4]:

$$\Omega_i = \{\mathbf{z} \mid (\mathbf{z} - \boldsymbol{\mu}_i)^T \boldsymbol{\Sigma}_i^{-1} (\mathbf{z} - \boldsymbol{\mu}_i) \le 1\}, \qquad (2)$$

where

$$\text{normalized pixel :} \quad \bar{\mathbf{x}}_j = \left[\frac{x_{r,j}}{A_r} \;\; \frac{x_{g,j}}{A_g} \;\; \frac{x_{b,j}}{A_b}\right]^T,$$

$$\text{mean vector :} \quad \boldsymbol{\mu}_i = \frac{1}{|\omega_i|} \sum_{j \in \omega_i} \bar{\mathbf{x}}_j = [\mu_{r,i} \;\; \mu_{g,i} \;\; \mu_{b,i}]^T,$$

$$\text{covariance matrix :} \quad \boldsymbol{\Sigma}_i = \frac{1}{|\omega_i|} \sum_{j \in \omega_i} (\bar{\mathbf{x}}_j - \boldsymbol{\mu})(\bar{\mathbf{x}}_j - \boldsymbol{\mu})^T = \begin{bmatrix} \sigma_{r,i}^2 & \sigma_{rg,i} & \sigma_{rb,i} \\ \sigma_{gr,i} & \sigma_{g,i}^2 & \sigma_{gb,i} \\ \sigma_{br,i} & \sigma_{bg} & \sigma_{b,i}^2 \end{bmatrix}.$$

In the RGB space, is located at the ellipsoid center, and determines the shape and orientation of the ellipsoid.

We proposed the color ellipsoid prior (CEP) vector as follows:

$$\theta_i = \min_{\mathbf{z} \in \Omega_i} \left\{ \min_{c \in \{r,g,b\}} z_c \right\}, \qquad (3)$$

Hereinafter, we calculate the CEP value directly from the ellipsoid geometry. We will drop the location subscript for clarity. Let each unit color component vector be , and . Denote for the plane perpendicular to the unit vector and passing through the origin. Then, is c-component value of and also the distance from to . Let be the vector minimizing the distance .

The closest to the plane is easily shown to be on the surface of . Then, the CEP value in (3) can be determined as follows:

The gradient direction of a vector on the ellipse surface is perpendicular to the tangent plane, and so the outward normal vector must have the same direction as the gradient of the ellipse surface. Thus,

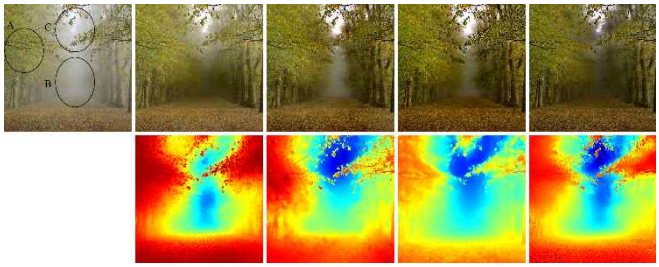

Fig. 4. Comparison of dehazed 'Forest' images and transmission maps. (a) Original image, (b) images dehazed by the DCP, (c) by the color-line, (d) by the haze-line, and (e) the proposed CEP.

$$\theta_i = \min_{\mathbf{z}\in\Omega_i}\left\{\min_{c\in\{r,g,b\}} z_c\right\} = \min_{c\in\{r,g,b\}}\left\{\min_{\mathbf{z}\in\Omega_i}\{\mathbf{e}_c^T\mathbf{z}\}\right\} = \min_{c\in\{r,g,b\}}\{\mathbf{e}_c^T\mathbf{z}_c^*\}, \quad (4)$$

where $S(\mathbf{z}_c^*) = (\mathbf{z}_c^* - \mu)^T\Sigma^{-1}(\mathbf{z}_c^* - \mu) = 1.$

$$\frac{\nabla_{\mathbf{z}}S(\mathbf{z}_c^*)}{\|\nabla_{\mathbf{z}}S(\mathbf{z}_c^*)\|} = -\mathbf{e}_c,$$

where the gradient is computed as [17]

$$\begin{aligned}\nabla_{\mathbf{z}}S(\mathbf{z}_c^*) &= \frac{d}{d\mathbf{z}}\left\{(\mathbf{z}-\mu)^T\Sigma^{-1}(\mathbf{z}-\mu)\right\}|_{\mathbf{z}=\mathbf{z}_c^*} \\ &= 2\Sigma^{-1}(\mathbf{z}_c^* - \mu).\end{aligned}$$

By replacing $\nabla_{\mathbf{z}}S(\mathbf{z}_c^*)$ with $2\Sigma^{-1}(\mathbf{z}_c^* - \mu)$,

$$\mathbf{z}_c^* - \mu = -\Sigma\mathbf{e}_c\|\Sigma^{-1}(\mathbf{z}_c^* - \mu)\|. \quad (5)$$

Then,

$$\begin{aligned}S(\mathbf{z}_c^*) &= (\mathbf{z}_c^* - \mu)^T\Sigma^{-1}(\mathbf{z}_c^* - \mu) \\ &= (\Sigma\mathbf{e}_c\|\Sigma^{-1}(\mathbf{z}_c^* - \mu)\|)^T\Sigma^{-1}(\Sigma\mathbf{e}_c\|\Sigma^{-1}(\mathbf{z}_c^* - \mu)\|) \\ \text{since } \Sigma^T &= \Sigma, \\ &= \|\Sigma^{-1}(\mathbf{z}_c^* - \mu)\|^2\mathbf{e}_c^T\Sigma\mathbf{e}_c = 1.\end{aligned}$$

2.2 Hallo artifact reduction by fuzzy segmentatio

We separate the heterogeneous patch ω_i into a set of foreground pixels ω_i^f and a set of background pixels ω_i^b. Then we denote Ω_i^b and Ω_i^f as the statistical ellipsoids constructed by ω_i^b and ω_i^f, respectively. To avoid transmission mismatches, the proposed method constructs the statistical ellipsoids from the pixels only in the region that

$$\theta_i = \min_{\mathbf{z}\in\Omega_i^*}\left\{\min_{c\in\{r,g,b\}} z_c\right\}, \quad (10)$$

where $\Omega_i^* = \begin{cases}\Omega_i^b, & \text{if } i \in \omega_i^b \\ \Omega_i^f, & \text{if } i \in \omega_i^f\end{cases}$

3. Experiments and discussion

We evaluate the existing competitive methods and the proposed method on the image dataset [10] that has been widely used. Moreresults are available at [11]. Fig. 11 compares the dehazed 'Forest' image and transmission maps from the proposed CEP, the DCP [2], the colorline [6], and the haze-line [9]. For the in-depth discussion, we specify three areas: a weakly hazy area (Area A), a deep forest area with dense haze (Area B. In Area A, the transmission values descend in order of the DCP, the CEP, the color-line method, and the haze-line method: and the dehazing performance strengths ascend in the same order. As the transmission values indicate, the hazeline method provides the strongest dehazing. The transmission values and the dehazing results from the CEP and the colorline method appear similar. Compared to other methods, the DCP results in insufficient dehazing because the pixels corresponding to the thin and dark branches make the transmission values large even though there are relatively few of these pixels.In Area B, because the haze is dense and there are not irregular pixels, the prior vectors by the CEP and the DCP are almost the same, so these methods reasonably reduce the dense haze. Meanwhile, the color-line and the haze-line methods produce insufficient dehazing. As seen in the transmission map, the color-line method invalidates the transmission values in this area and interpolates the values from surrounding areas, such as the sky or ground, causing the values not to be too small to dehaze the area effectively. Since haze-free pixels do not exist in Area B, the prior vector selected by the haze-line method is close to atmospheric light, making the transmission value large and prohibiting the method from fully reducing the dense haze. The CEP and the DCP generate transmission maps that distinguish Area B and the surrounding tree regions, whereas the maps generated by the color-line method and the haze-line method rarely outline the deep forest region. From these results, the CEP renders more of the forest in the dehazed images, compared to the other methods.

감사의 글

본 연구는 산업통상원부의 재원으로 수행되었음 (10067205 , 화재현장의 농연환경 내 가시거리 확장을 위한 영상센서모듈 개발)

This leads to,

$$\|\Sigma^{-1}(\mathbf{z}_c^* - \mu)\| = \frac{1}{\sqrt{\mathbf{e}_c^T \Sigma \mathbf{e}_c}} = \frac{1}{\sigma_c}. \quad (6)$$

From (5) and (6), the minimum distance from a vector of Ω_i to plane $\mathbf{H}_c$ is

$$\mathbf{e}_c^T \mathbf{z}_c^* = \mathbf{e}_c^T \left(\mu - \frac{1}{\sigma_c} \Sigma \mathbf{e}_c \right) = \mu_c - \sigma_c. \quad (7)$$

Then, the proposed CEP value is obtained as

$$\theta_i = \min_{c \in \{r,g,b\}} \{\mathbf{e}_c^T \mathbf{z}_c^*\} = \min_{c \in \{r,g,b\}} \{\mu_{c,i} - \sigma_{c,i}\}. \quad (8)$$

Therefore, the CEP transmission estimator becomes

$$t_i = 1 - \alpha\ \theta_i = 1 - \alpha \min_{c \in \{r,g,b\}} \{\mu_{c,i} - \sigma_{c,i}\}. \quad (9)$$

References

[1] R. Fattal, "Single image dehazing", ACM Trans. Graph, vol. 27, no. 3, pp. 72, 2008.

[2] K. He, J. Sun, and X. Tang, "Single image haze removal using dark channel prior", IEEE Trans. Pattern Anal. and Mach. Intell., vol. 33, no. 12, pp. 2341 - 2353, Dec. 2011.

[3] K.B. Gibson, D.T. Vo, and T.Q. Nguyen, "An investigation of dehazing effects on image and video coding", IEEE Trans. on Image Processing, vol. 21, no. 2, pp. 662 - 673, Feb. 2012.

[4] K.B. Gibson and T.Q. Nguyen, "An analysis of single image defogging methods using a color ellipsoid framework", EURASIP Journal on Image and Video Processing, vol. 2013, no. 1, pp. 1 - 14, 2013.

[5] G. Meng, Y. Wang, J. Duan, S. Xiang, and C. Pan, "Efficient image dehazing with boundary constraint and contextual regularization", IEEE Intl Conf. Computer Vision, 2013.

[6] R. Fattal, "Dehazing using color-lines", ACM Trans. Graph, vol. 34, no. 1, 2014.

[7] K. Tang, J. Yang, and J. Wang, "Investigating haze-relevant features in a learning framework for image dehazing", IEEE Conf. Computer Vision and Pattern Recognition, 2014.

[8] B. Cai, X. Xu, K. Jia, C. Qing, and D. Tao, "Dehazenet: An end-to end system for single image haze removal", IEEE Trans. on Image Processing, vol. 25, no. 11, pp. 5187 - 5198, Nov. 2016.

[9] D. Berman, T. Treibitz, and S. Avidan, "Non-local image dehazing", IEEE Conf. Computer Vision and Pattern Recognition, 2016.

[10] Hazy image dataset [Online], Available: http://www.cs.huji.ac.il/ raananf/projects/dehaze cl/results/.

[11] Dehazing results by Color Ellipsoid Prior [Online], Available: https://github.com/mtbui2010/CEP/.